Syntheses and characterizations of iridium complexes containing bidentate phosphine ligands and their catalytic hydrogenation reactions to α,β-unsaturated aldehydes

Rui-Xiang Li[a], Xian-Jun Li[a,*], Ning-Bew Wong[b], Kam-Chung Tin[b], Zhong-Yuan Zhou[c], Thomas C.W. Mak[c]

[a] *Department of Chemistry, Sichuan University, Chengdu, Sichuan, China*
[b] *Department of Biology and Chemistry, City University of Hong Kong, Tat Chee Avenue, Kowloon, Hong Kong, China*
[c] *Department of Chemistry, Chinese University of Hong Kong, Shatin, NT, Hong Kong, China*

Abstract

Five iridium complexes containing bidentate phosphine ligands, IrH(CO)(PPh$_3$)(BPPB) [BPPB = 1,2-bis(diphenyl-phosphino)benzene] (**1**), IrH(CO)(PPh$_3$)(BISBI) [BISBI = 2,2′-bis(diphenylphosphinomethyl)-1,1′-biphenyl] (**2**), IrH(CO)(PPh$_3$)(BDNA) [BDNA = 1,8-bis(diphenylphosphinomethyl)naphthalene] (**3**), IrH(CO)(PPh$_3$)(BDPX) [BDPX = 1,2-bis(diphenylphosphinomethyl)benzene] (**4**), and IrHCl(CO)(PCP) [PCP-H = 1,3-bis(diphenylphosphinomethyl)benzene] (**5**) were synthesized. Their compositions and structures were identified by elemental analysis, FTIR, ^{31}P{^{1}H} NMR and ^{1}H NMR. The molecular structure of IrH(CO)(PPh$_3$)(BDNA) determined by single crystal X-ray diffraction indicated a trigonal bipyramidal structure with the three phosphorus atoms in the equatorial plane. The crystal belonged to triclinic system, *P1* space group, $a = 11.47$ Å, $b = 11.65$ Å, $c = 19.20$ Å, $\alpha = 81.95°$, $\beta = 75.60°$, $\gamma = 70.60°$, and $Z = 2$. The catalytic hydrogenation activities and selectivities of the five complexes as catalysts for citral and cinnamaldehyde were investigated. Complexes **1**–**4** showed high selectivity for the hydrogenation of C=O group in citral. High selectivity for the hydrogenation of C=O group in cinnamaldehyde catalyzed by complex **4** could be obtained in the presence of excess amount of ligand (BDPX). © 2002 Elsevier Science B.V. All rights reserved.

Keywords: Iridium complex; Bidentate phosphine; Hydrogenation; Citral; Cinnamaldehyde

1. Introduction

In recent years, a great number of ruthenium and rhodium complexes with bidentate phosphines were synthesized and characterized. These complexes generally exhibited better activities and selectivities for hydrogenation and hydroformylation of unsaturated substrates than the analogous monophosphine com-

plexes [1–7]. Although iridium complexes generally exhibit lower catalytic hydrogenation activities for unsaturated compounds than ruthenium and rhodium complexes, the iridium-phosphine complexes usually exhibit very good selectivity for the hydrogenations of α,β-unsaturated ketones [8–12] and α,β-unsaturated aldehydes [13–16] under optimum reaction conditions. However, the studies on syntheses and catalytic reactions of iridium complexes containing bidentate phosphines are still very scarce [17–20]. The hydrogenation of carbonyl group of an organic compound

* Corresponding author. Fax: +86-28-5412006.
E-mail address: scuulixj@mail.sc.cninfo.net (X.-J. Li).

catalyzed by transition metal complex is more difficult than hydrogenation of an olefinic group; therefore, it is still a challenging problem to synthesize highly selective catalysts for the hydrogenation of carbonyl group in α,β-unsaturated carbonyl compounds. In this paper, we would like to report a simplified method for synthesizing 1,2-bis(diphenylphosphinomethyl)benzene (BDPX) [21], a modified method for preparing IrH(CO)(PPh₃)(BISBI) [2,2′-bis(diphenylphosphinomethyl)-1,1′-biphenyl] with high purity and yield [22] and the syntheses of four new iridium complexes containing biphosphine ligands with different chelating ring sizes (Fig. 1). The effect of coordination environment on hydrogenation activities and selectivities

for the carbonyl group of citral and cinnamaldehyde were also discussed.

2. Experimental

2.1. Materials

All synthetic reactions were performed with standard Schlenk technique under nitrogen atmosphere. Solvents were dried over appropriate drying agents and distilled under nitrogen prior to use. Reagent-grade PPh₃, 1,3-bis(bromomethyl)benzene and 1,2-bis(bromomethyl)benzene were purchased
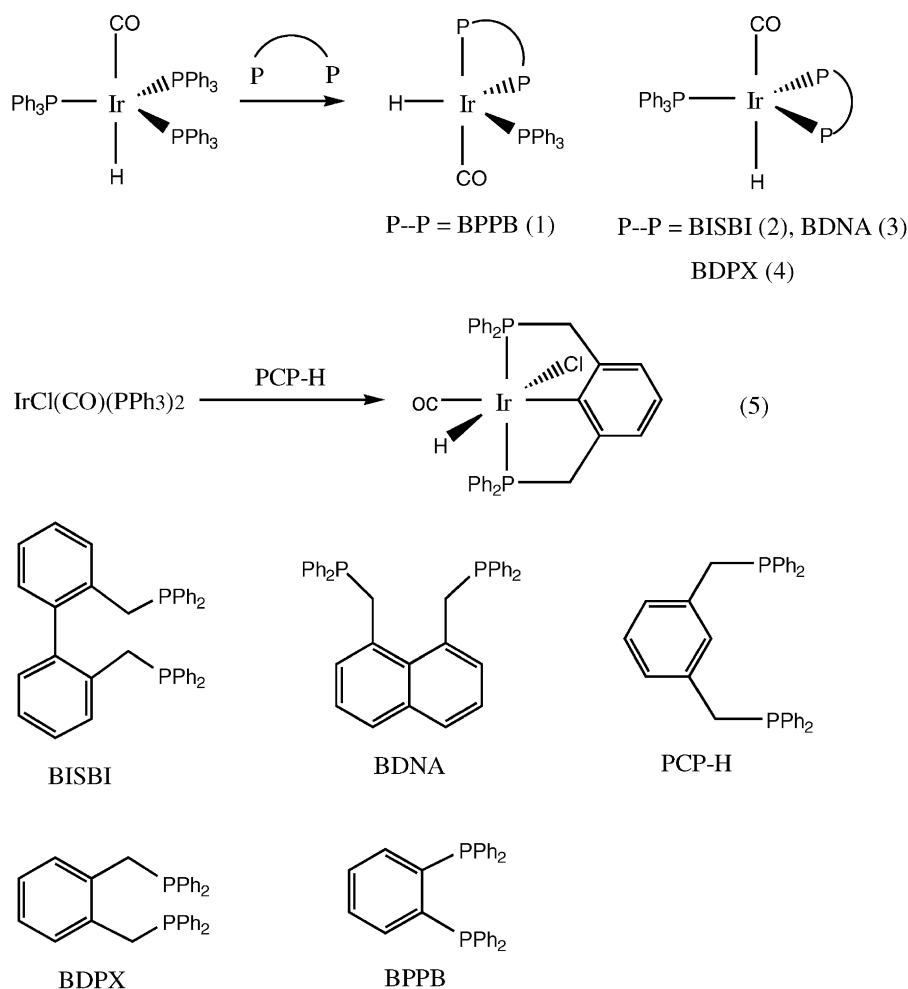

Fig. 1. Structures of ligands and complexes.

from Aldrich. BPPB [1,2-bis(diphenylphosphino) benzene] was from Strem, and $IrCl_3 \cdot HCl \cdot xH_2O$ was from Kunming Nobel Metals, China. Citral (97%) and cinnamaldehyde (98%) from Riedel-deHaen were distilled before use. Starting materials $IrH(CO)(PPh_3)_3$, $Ir(CO)Cl(PPh_3)_2$ [23], PCP-H [1,3-bis(diphenylphosphinomethyl)benzene] [24], BISBI [25] and BDNA [1,8-bis(diphenylphosphinomethyl)naphthalene] [7] were prepared according to the reported methods.

2.2. Analytical methods

The ^1H and $^{31}P\{^1H\}$ NMR spectra in $CDCl_3$ were recorded on a Bruker ARX 300 spectrometer at room temperature, at 300 MHz for ^1H NMR with TMS as internal standard and at 121.5 MHz for $^{31}P\{^1H\}$ NMR with 85% H_3PO_4 as external standard, with downfield shifts as positive. Elemental analyses were performed by Shanghai Institute of Organic Chemistry, Chinese Academy of Sciences. FTIR was recorded on a Perkin Elmer 1600 spectrometer with KBr plates.

2.3. Catalytic hydrogenation

Appropriate amount of catalyst and substrate were introduced into a stainless steel autoclave (100 ml) equipped with a stirrer (Parr 4561 minireactor). The autoclave was evacuated and flushed consecutively with high purity hydrogen (99.995%) for five times, then filled with the hydrogen to the desired pressure. After the reaction mixture was heated to the desired temperature, stirring was started (400 rpm) and reaction time was accounted. The reaction was quenched by immersing the reactor in an ice-bath. The products were analyzed on a GC (HP 5890 Series II) with FID and a capillary column (HP-FFAP, 25 m × 0.2 mm × 0.33 μm), and the GC graphs were obtained with an HP 3396 Integrator. The components were identified by authentic samples on GC and GC-MS (HP 5890 GC with series mass selective detector).

3. Preparation of ligand and complexes

3.1. 1,2-Bis(diphenylphosphinomethyl)benzene (BDPX)

Triphenylphosphine 7.9 g (30 mmol) and lithium 0.45 g (65 mmol) in 30 ml THF were stirred for 3 h

at room temperature, and the orange-red solution was filtered to remove the unreacted lithium. *t*-Butyl chloride 2.5 g (27 mmol) in 10 ml THF was slowly added to the filtrate cooling in an ice-bath, and then the solution was heated to reflux for 10 min. The solution was cooled to 0 °C in an ice-bath again, and 1,2-bis(bromomethyl)benzene 3.6 g (13.6 mmol) in 20 ml THF was added slowly into the cooled solution over a period of 50 min, while the color of the solution changed from orange-red to pale yellow. The reaction mixture was heated to reflux for 30 min before the solvents were evaporated to give a yellow sticky solid under vacuum. CH_2Cl_2 (30 ml) and water (20 ml) were added to dissolve the solid, and then it was allowed to separate in a separatory funnel. The organic layer was collected and reduced to ca. 10 ml under vacuum. Ethanol (30 ml) was added to the CH_2Cl_2 solution, and a lot of white needle crystals were formed immediately. The product was filtered, washed with ethanol and dried under vacuum to give BDPX as white needles; mp: 125–126 °C.

3.2. Complex 1

$IrH(CO)(PPh_3)_3$ 0.101 g (0.1 mmol) and BPPB 0.046 g (0.1 mmol) were dissolved in 10 ml toluene. The color of the solution changed eventually to orange-red during reflux. The 20 ml *n*-hexane was added to the reaction solution and caused the formation of orange-red precipitates after 2 h. The product was filtered, washed with diethyl ether and dried under vacuum to give orange-red powder.

3.3. Complexes 2–5

$IrH(CO)(PPh_3)_3$ 0.080 g (0.08 mmol) and BISBI 0.045 g (0.08 mmol) were dissolved in 10 ml toluene. The yellow solution was refluxed for 3 h, and then was concentrated to ca. 2 ml under vacuum. The addition of 20 ml *n*-hexane to the solution caused the formation of yellow precipitates. The product was filtered, washed with diethyl ether and dried under vacuum to give yellow powder. The preparation procedures of complexes 3–5 were the same as complex 2, but complex 5 was formed by using $IrCl(CO)(PPh_3)_2$ as starting materials.

The elemental analysis, NMR and FTIR of all complexes were listed in Tables 1–3, respectively. $^{31}P\{^1H\}$

Table 1
Elemental analysis data of BDPX and all complexes

Ligand or complex	Calculated		Found		Yield
	C (%)	H (%)	C (%)	H (%)	
BDPX for $C_{32}H_{28}P_2$	81.00	5.95	81.23	5.86	4.2 (65%)
1 for $C_{49}H_{40}OP_3Ir$	63.30	4.36	63.21	4.37	0.070 (75%)
2 for $C_{57}H_{48}OP_3Ir$	66.20	4.68	66.16	4.69	0.075 (92%)
3 for $C_{55}H_{46}OP_3Ir$	65.53	4.60	65.48	4.77	0.046 (47%)
4 for $C_{51}H_{44}OP_3Ir$	63.94	4.63	63.85	4.65	0.065 (68%)
5 for $C_{33}H_{28}ClOP_2Ir$	54.21	4.00	54.71	3.95	0.095 (66%)

NMR of complex **4** showed widened multi-peaks at 20.70 ppm and widened doublet at 0.04 ppm with indeterminable coupling constants at room temperature. When temperature was decreased to −50 °C, two sets of peaks were observed and the intensity ratio of the stronger peaks to the weaker peaks was ca. 2:1. The weaker peaks were a doublet at 0.37 ppm and a triplet at 19.82 ppm with $J_{P-P} = 109.6$ Hz. The stronger peaks were a doublets at −0.52 ppm and a triplet at 20.86 ppm with $J_{P-P} = 115.9$ Hz. ^{1}H NMR: a widened asymmetric multiplet at −11.65 ppm which could further split into indeterminable multiplets at −50 °C.

3.4. X-ray crystallographic analysis of IrH(CO)(PPh3)(BDNA)·1/2CH3COCH3

The yellow prism crystal was grown in acetone. The crystal (0.20 mm × 0.20 mm × 0.16 mm) covered with a thin layer of paraffin oil as a precaution against decomposition in air was mounted on a Rigaku RAXIS IIC imaging-plate diffractometer

Table 3
FTIR spectra of complexes

Complex	ν_{CO}	ν_{Ir-H}
1	1911.3 (s)	2032.1 (m)
2	1926.3 (s)	2067.1 (m)
3	1933.3 (s)	2093.1 (m)
4	1931.4 (s)	2056.8 (m)
5	2018.0 (s)	2183.0 (m)

with a rotating-anode generator powered at 50 kV and 90 mA. Intensity data were collected at 294 K using graphite-monochromatized Mo Kα radiation ($\lambda = 0.7103$ Å) by taking 53 oscillation photos in the range of 0–150°, $\Delta\phi = 3°$, and exposing time was 8 min per frame. Crystal-to-detector distance was 78.10 mm and background level was −40. The θ range for data collection was 1.10–22.72°. A self-consistent semi-empirical absorption correction was applied using ABSCOR program. All calculation were performed with Siemens SHELXTL PLUS (PC Version) system. Structure refinement was based on

Table 2
NMR spectra of complexes

Complex	^{1}H NMR	^{31}P{^{1}H} NMR
BDPX	3.3 (4H, s), 6.9–7.3 (24H, m)	−12.3 (s)
1	−10.9 (dt), $J_{P1,2-H} = 39$, $J_{P3-H} = 24$	39.3 (d), 10.6 (t), $J_{P-P} = 44$
2	−11.5 (dt), $J_{P1,2-H} = 24$, $J_{P3-H} = 15$ $J_{Pa-Px} = 123$, $J_{Px-Pb} = 120$	14.39 (dd), 13.63 (dd), 9.74 (dd), $J_{Pa-Pb} = 120$,
3	−11.9 (dt), $J_{P1,2-H} = 21$, $J_{P3-H} = 17$	21.5 (t), 13.0 (d), $J_{P-P} = 113$
4[a]	−11.65 (m)	19.82 (dd), 0.37 (dt), $J_{P-P} = 109.6$ 20.86 (dd), −0.52 (dt), $J_{P-P} = 115.9$
5	−17.74 (t), $J_{P-H} = 13.5$	25.07 (s)

[a] The spectrum was recorded at −50 °C.

Table 4
Crystal data and structure refinement for complex **3**

Empirical formula	$C_{57}H_{46}IrOP_3$
Formula weight	1032.05
Temperature	293(2) K
Wavelength	0.71073 Å
Crystal system	Triclinic
Space group	*P1*
Unit cell dimensions	$a = 11.468(2)$ Å, $\alpha = 81.95(3)°$
	$b = 11.647(2)$ Å, $\beta = 75.60(3)°$
	$c = 19.197(4)$ Å, $\gamma = 70.60(3)°$
Volume	2337.9(8) Å^3
Z	2
Density (calculated)	1.466 mg/cm^3
Absorption coefficient	2.998 mm^{-1}
Transmission factor	0.742–1.000
$F(0\,0\,0)$	1036
Crystal size	0.20 mm × 0.20 mm × 0.16 mm
θ range for data collection	1.10–22.72°
Index ranges	$-12 \leq h \leq 11$, $-12 \leq k \leq 0$,
	$-20 \leq l \leq 20$
Reflections collected	5695
Independent reflections	5695 ($R_{\text{int}} = 0.0000$)
Maximum and minimum transmission	0.6455 and 0.5854
Refinement method	Full-matrix least-squares on F^2
Data/restraints/parameters	5695/27/1273
Goodness-of-fit on F^2	1.453
Final R indices [$I > 2\sigma(I)$]	R1 = 0.0568, $wR2 = 0.1522$
R indices (all data)	R1 = 0.0572, $wR2 = 0.1528$
Absolute structure parameter	0.019 (9)
Extinction coefficient	0.00500 (17)
Largest differential peak and hole	0.604 and -0.763 eÅ^{-3}

F^2 for all reflections. A final R-factor was 0.0568 ($wR = 0.1522$). Crystallographic data were summarized in Table 4.

4. Results and discussion

4.1. Preparation of BDPX

The ligand BDPX was very sensitive to air oxidation in solution, but quite stable in solid form. It was generally synthesized by reacting α,α′-dichloro-*o*-xylene with NaPPh$_2$ in liquid ammonia [21]. This was a tedious procedure with unsatisfactory yield (46%). According to the modified method of reacting triphenylphosphine with lithium in THF at room temper-

ature, the preparation of BDPX was much easier in addition to a better yield (62%).

4.2. Structures of complexes **2**–**4**

Complexes **1**–**4** were air sensitive in solution and in solid state. For complex **1**, the intensity ratio of the doublet at 39.16 ppm to the triplet at 10.56 ppm was about 2:1 in ^{31}P{^{1}H} NMR spectrum. The small coupling constant ($J_{\text{P–P}} = 44$ Hz) indicated that the all phosphorus were in *cis*-position to each other. Since the coupling constant between the phosphines in an equatorial sites is generally more than 100 Hz and is much larger than that between the phosphines in an equatorial and an apical site [26], the small coupling constant supports one phosphorus atom in an apical site and two phosphorus atoms in an equatorial site. BPPB is of a similar natural bite angle with DIPHOS (1,2-bis(diphenylphosphino)ethane); the small natural bite angle (85°) of DIPHOS leads to the structure where one phosphorus atom occupies an equatorial site and another phosphorus atom occupies an apical site in the triangle bipyramidal structure. Similarly, one phosphorus atom in BPPB should occupy an apical site and another phosphorus atom should occupy an equatorial site in complex **1**. ^{1}H NMR spectrum showed a doublet of triplet with the small P–H coupling constants ($J_{\text{P1,2-H}} = 39$ Hz, $J_{\text{P3-H}} = 24$ Hz) for the coordinated hydride. Therefore, it was reasonable to deduce that the hydride was in *cis*-position to all three phosphorus atoms. The proposed molecular structure was shown in Fig. 1. The small coupling constants and the splitting pattern in NMR spectra indicated that a fact fluxional process occurred at room temperature. The fluxional process was probably a Berry pseudorotation [26] (Fig. 2).

Complex **2** was originally synthesized by Casey et al. [22]. We had modified the method to give a high purity and good yield product without recrystallization. Its ^{1}H NMR spectrum showed a doublet of triplet at -11.48 ppm with the small coupling constants ($J_{\text{P1,2-H}} = 24$ Hz and $J_{\text{P3-H}} = 15$ Hz). Although the PPh$_3$ in complex **2** showed a doublet of doublets at 9.74 ppm in ^{31}P{^{1}H} NMR, the phosphorus atoms of BISBI exhibited two doublets of doublets at 14.39 and 13.63 ppm. This spectrum was consistent with the ABX splitting pattern. The much larger P–P coupling constant indicated that all phosphorus
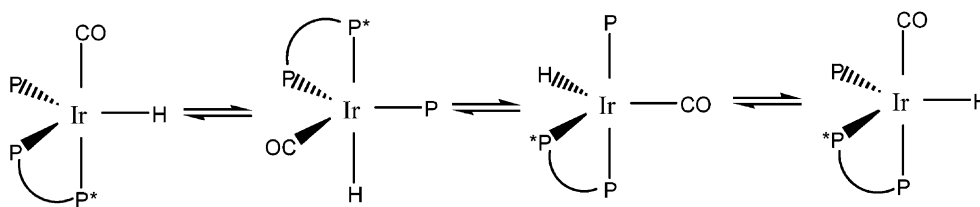
Fig. 2. Berry peseudorotation of complex **1**.

atoms were in equatorial plane If the difference of the chelating ring was omitted, the steric structure of this complex was shown in Fig. 1.

^{1}H NMR spectrum of complex **3** showed doublet of triplets at −11.93 ppm with $J_{P1,2-H} = 21$ Hz and $J_{P3-H} = 17$ Hz, and ^{31}P{^{1}H} NMR spectrum showed a doublet at 12.96 ppm and a triplet at 21.52 ppm with $J_{P-P} = 113$ Hz. Thus, the much large coupling constant supported that the steric structure of complex

3 should be similar to complex **2** (Fig. 1). The proposed structure was also confirmed by the single crystal X-ray diffraction (Fig. 3).

The results of X-ray diffraction of complex **3** was listed in Tables 4 and 5, and Fig. 3. The structure was consistent with the structural analysis by NMR. However, the elemental analysis indicated that an acetone molecule contained in the crystal cell was removed under vacuum. The rigid naphthalene ring limited the
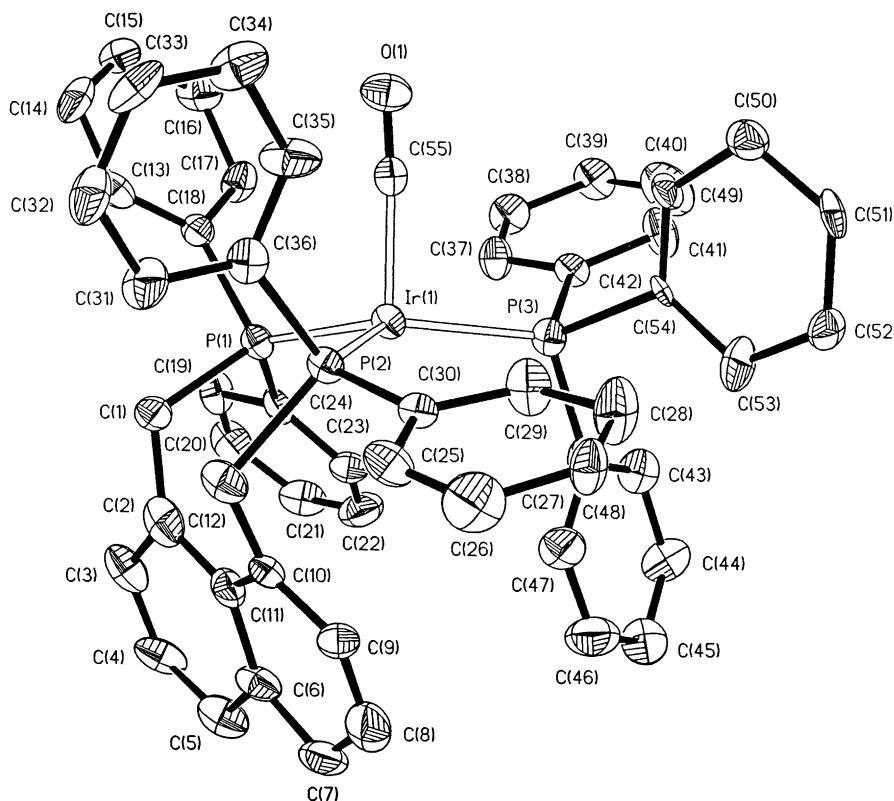

Fig. 3. An ORTEP drawing of complex **3**.

Table 5
Selected bond lengths (Å) and bond angles (°)

Bonds	Length (Å) or angle (°)
Ir–C(55)	1.912 (3)
Ir–P(1)	2.2444 (10)
Ir–P(2)	2.3458 (9)
Ir–P(3)	2.2762 (11)
C(55)–Ir–P(1)	97.57 (8)
C(55)–Ir–P(2)	104.95 (9)
C(55)–Ir–P(3)	93.64 (8)
P(1)–Ir–P(2)	103.98 (4)
P(1)–Ir–P(3)	124.69 (3)
P(2)–Ir–P(3)	124.85 (4)
C(2)–C(11)–C(10)	127.3 (3)
C(5)–C(6)–C(7)	109.1 (3)

chelating angle of P(1)–Ir–P(2) to 103.98°, which was much smaller than 120°. As a result, 124.69° of P(1)–Ir–P(3) and 124.85° of P(2)–Ir–P(3) were larger than 120°. The 97.58° of C(55)–Ir–P(1), 104.95° of C(55)–Ir–P(2) and 104.95° of C(55)–Ir–P(3) indicated that phosphine ligands were close to the hydride in the *trans*-position of carbonyl in order to reduce the tension caused by the interaction between the carbonyl group and the phosphine ligands. Therefore, Ir did not located in the plane formed by P(1), P(2) and P(3). Because of the distorted tension force, the bond angle of C(2)–C(11)–C(10) (127.3°) was larger than 120°, and that of C(5)–C(6)–C(7) (109.1°) was smaller than 120°.

The structural property of the complex **4** was different from the previous complexes. ^{31}P$\{^1$H$\}$ NMR showed two wide peaks at about 0.04 and 20.70 ppm at room temperature. When the temperature was decreased to −50 °C, the two wide peaks were sharpened and split, the broad peak at 20.70 ppm was transformed into two triplets which were centered at 20.86

and 19.82 ppm, and the wide peak at 0.04 ppm was split into two doublets which were centered at 0.37 and −0.52 ppm. The results strongly indicated that the complex was composed of two isomers and they could be converted to each other in solution at room temperature. The intensity ratio of the weaker set of peaks at 19.82 and 0.37 ppm to the stronger set of peaks at 20.86 and −0.52 ppm was ca. 1–2. The hydride in ^{1}H NMR spectrum appeared as a widened unsymmetric multiplet at −11.65 ppm which was further split into overlapping multiplet as temperature was decreased to −50 °C. The absence of large H–P coupling constant in ^{1}H NMR spectrum had indicated that the hydride was in the *cis*-position to all phosphine ligands. Since the two isomers showed the same splitting pattern and the close coupling constant in NMR spectra, it indicated that the chemical environments of phosphorus atoms could not be very different. We deduced that the difference was from the transformation of the backbone in bidentate ligand (Fig. 4). The major isomer should be B because the stero hindrance between hydrogen atom and bidentate ligand in structure B was smaller than in structure A.

4.3. Structure of complex 5

An equimolar mixture of IrCl(CO)(PPh$_3$)$_2$ and ligand (PCP-H) was refluxed in toluene to produce the yellow complex IrHCl(CO)(PCP). The singlet of ^{31}P$\{^1$H$\}$ NMR spectrum at 25.07 ppm showed that the two phosphorus atoms of PCP were equilvalent and occupied the two apical positions of the octahedron. The triplet of a hydride at −17.74 ppm in ^{1}H NMR spectrum confirmed that the orthometallation reaction had happened and the hydride was in *cis*-position to two phosphorus atom. The orthometallation occurred by the oxidation addition of C–H bond in the phenyl
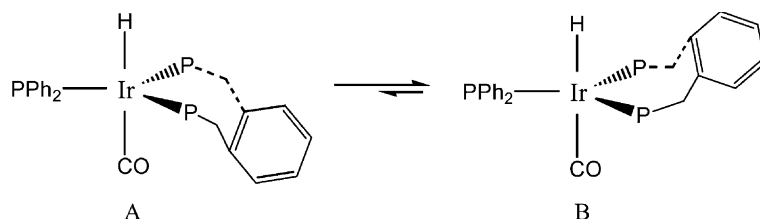

Fig. 4. Structural transformation of complex **4**.

ring of the ligand to iridium during the reaction. It has been extensively observed that the bisphosphine ligands 1,3-$(R_2PCH_2)_2C_6H_4$, where R = Bu^t, Ph, Cy, Me and Et, could undergo cyclometallation reactions with Ni, Pd, Pt, Rh, Ru and Ir to form complexes of tridentate $[(2,6-(R_2PCH_2)_2C_6H_3)^-]$ [24,27–29]. The NMR spectra of the complex was consistent with an octahedron structure. Since H$^-$ and C$^-$ in benzene ring have a stronger *trans*-influence than Cl$^-$ and CO, structure of complex **5** was proposed as shown in Fig. 1.

4.4. IR spectra of complexes

Compared with the analogous iridium complex with triphenylphosphine, the IR absorption peak of the carbonyl group in complex **1** shifted to the lower wavenumber 1911 cm^{-1} and the carbonyl absorption of complexes **2**–**4** shifted to higher wavenumber 1926, 1933 and 1931 cm^{-1}, respectively. The data suggested that more d electron of iridium in complex **1** was back-donated to π* orbital of CO than in IrH(CO)(PPh$_3$)$_3$. The result was consistent with the proposed structure because a strong electron-donating ligand coordinated to the *trans*-position of CO and led to a more back-donating electron transforming to π* orbital of CO. In contrast, the back-donating electron to π* orbital of CO from iridium in complexes **2**–**4** were less than in IrH(CO)(PPh$_3$)$_3$. The high wavenumber (2018 cm^{-1}) of carbonyl group in complex **5** revealed that iridium was in higher

oxidation state and the back-donating electron from iridium(III) to π* orbital of carbonyl was less. The high wavenumber (2183 cm^{-1}) of Ir–H bond also revealed that the bonding between iridium and hydride was stronger in Ir(III) than Ir(I) complex.

4.5. Hydrogenation of citral and cinnamaldehyde by iridium complexes

The hydrogenation routes and results of citral and cinnamaldehyde were shown in Table 6 and Fig. 5. When two triphenylphosphines in IrH(CO)(PPh$_3$)$_3$ were replaced with a bidentate phosphine, all complexes exhibited higher catalytic activities than the analogous complex with triphenylphosphine. Among these complexes, the complex **4** exhibited the highest catalytic activity and selectivity for the hydrogenation of carbonyl group in citral. The selectivities of complexes **2**–**4** to form allylic alcohol were over 92%. However, all complexes showed unsatisfactory selectivity for the hydrogenation of cinnamaldehyde to form cinnamyl alcohol. According to the results in Table 6, complex **4** showed the highest activities for the hydrogenations of citral and cinnamaldehyde. This result was perhaps related to its ligand structure.

The selectivity for the hydrogenation of cinnamaldehyde to form cinnamyl alcohol using these complexes as catalysts were unsatisfactory with the formation of saturated aldehyde (phenylpropanal). When cinnamyl alcohol was used as substrate under the similar reaction conditions, the saturated aldehyde,

Table 6
Catalytic hydrogenation of α,β-unsaturated aldehydes[a]

Complexes	Citral[b]		Cinnamaldehyde[c]	
	Conversion (%)	Selectivity (%)[c]	Conversion (%)	Selectivity (%)[d]
IrH(CO)(PPh$_3$)$_3$	3.1	70.5	11.4	35.0
IrH(CO)(PPh$_3$)(BPPB)	7.7	61.2	27.3	19.3
IrH(CO)(PPh$_3$)(BISBI)	11.6	92.2	44.6	13.1
IrH(CO)(PPh$_3$)(BDNA)	19.3	95.8	20.6	77.4
IrH(CO)(PPh$_3$)(BDPX)	58.8	96.4	58.1	9.0
IrHCl(CO)(PCP)	13.9	42.5	52.0	1.3

[a] Reaction conditions: H$_2$ pressure 50 kg/cm^2, catalyst concentration 1.0×10^{-3} M, citral or cinnamaldehyde 2.0 ml, toluene 8.0 ml, temperature 100 °C.
[b] Reaction time: 5 h.
[c] Reaction time: 3 h.
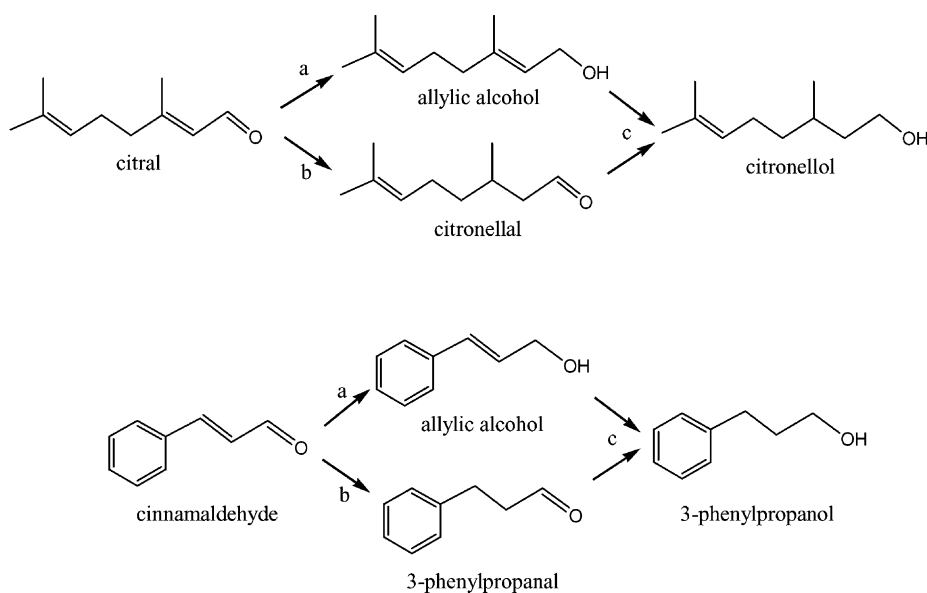[d] Allylic alcohol.

Fig. 5. Hydrogenation routes of citral and cinnamaldehyde.

Table 7
Hydrogenation of cinnamaldehyde in the presence of IrH(CO)(PPh$_3$)(BDPX) and BDPX ligand[a]

Ligand/complex (molar ratio)	Conversion (%)	Distribution of products (%)		
		Phenylpropanal	Phenylpropanol	Cinnamyl alcohol
0[b]	58.1	72.6	18.3	9.0
1	70.9	67.0	19.8	13.2
2	20.9	6.1	7.5	86.4
5	24.4	3.3	4.5	92.2

[a] Reaction conditions: reaction time 5 h, others were same as in Table 3.
[b] Reaction time: 3 h.

which could be formed by the isomerization of the double bond in cinnamyl alcohol, was not detected in the reaction products. This result indicated that the hydrogenation of cinnamaldehyde to form phenylpropanal occurred directly on the C=C double bond rather than on the C=O bond to form cinnamyl alcohol followed by its isomerization to the saturated aldehyde as reported by Chin et al. [16].

When the complex **4** was used as catalyst in the presence of larger excess BDPX (Ir/BDPX = 5:1 in Table 7), the hydrogenation reaction of the C=C in cinnamaldehyde could be greatly suppressed, so that a much higher selectivity for cinnamyl alcohol was obtained. These results were in agreement with the mechanisms in which an active species with two phosphorus atoms complex was responsible for C=C bond reduction, whereas carbonyl group reduction was related to a species with three coordinated phosphorus atoms [30,31] because the high ratio of BDPX to Ir was favorable for the formation of the species with three coordinated phosphorus atoms.

References

[1] B.R. James, A. Pacheco, S.J. Rettig, J. Mol. Catal. 14 (1987) 147.
[2] R. Noyori, H. Takaya, Acc. Chem. Res. 23 (1990) 345.

[3] S.A. King, S.A. Thompson, K.O. King, T.R. Verhoeven, J. Org. Chem. 57 (1992) 6689.

[4] A. Mezzetti, G. Consiglio, J. Chem. Soc., Chem. Commun. (1991) 1675.

[5] A.S.C. Chan, W. Hu, C.C. Pai, C.P. Lau, Y. Jiang, A. Mi, M. Yan, J. Sun, R. Lou, J. Deng, J. Am. Chem. Soc. 119 (1997) 9570.

[6] R.X. Li, K.C. Tin, N.B. Wong, Z.Y. Zhang, T.C.W. Mak, X.J. Li, J. Organomet. Chem. 557 (1998) 207.

[7] R.X. Li, N.B. Wong, X.J. Li, T.C.W. Mak, Q.C. Yang, K.C. Tin, J. Organomet. Chem. 571 (1998) 223.

[8] E. Farnetti, M. Pesce, J. Kaspar, R. Spogliarich, M. Graziani, J. Chem. Soc., Chem. Commun. (1986) 746.

[9] K. Mashima, T. Akutagawa, X. Zhang, H. Takaya, T. Taketomi, H. Kumobayashi, H. Akutagawa, J. Organomet. Chem. 428 (1992) 213.

[10] E. Farnetti, G. Nardin, M. Graziani, J. Organomet. Chem. 417 (1991) 163.

[11] E. Farnetti, J. Kaspar, R. Spogliarich, M. Graziani, J. Chem. Soc., Dalton Trans. (1988) 947.

[12] R. Spogliarich, E. Farnetti, J. Kaspar, M. Grazian, E. Cesarotti, J. Mol. Catal. 50 (1989) 19.

[13] R.S. Coffey, J. Chem. Soc., Chem. Commun. (1967) 923.

[14] B.R. James, R. Morris, J. Chem. Soc., Chem. Commun. (1978) 929.

[15] W. Strohmeier, H. Steigerwald, J. Organomet. Chem. 129 (1997) C43.

[16] C.S. Chin, B. Lee, S.C. Park, J. Organomet. Chem. 393 (1990) 131.

[17] R.C. Schnabel, P.S. Carroll, D.M. Roddick, Organometallics 15 (1996) 655.

[18] H.A. Mayer, R. Fawzi, M. Steimann, Chem. Ber. 126 (1993) 1341.

[19] C.A. Miller, T.S. Janik, C.H. Lake, L.M. Toomey, M.R. Churchill, J.D. Atwood, Organometallics 13 (1994) 5080.

[20] J.H. Holloway, E.G. Hope, D.R. Russell, G.C. Saunders, Polyhedron 15 (1996) 173.

[21] M. Camalli, F. Caruso, S. Chaloupka, E.M. Leber, H. Rimml, L.M. Venanzi, Helv. Chim. Acta 73 (1990) 2263.

[22] C.P. Casey, T.G. Whiteker, M.G. Melville, L.M. Petrovich, J.A. Gavney, D.R. Powell, J. Am. Chem. Soc. 114 (1992) 5535.

[23] J.J. Levison, D. Robinson, J. Chem. Soc. A (1970) 2947.

[24] H. Rimml, L.M. Venanzi, J. Organomet. Chem. 259 (1983) C6.

[25] T.W. Puckertte, T.J. Devon, G.W. Phillips, J.L. Stavinoha, US Patent (1989) 4879416; Chem. Abstr. 112 (1989) 217269k.

[26] C.P. Casey, E.L. Paulsen, E.W. Beuttenmueller, B.R. Proft, L.M. Petrovich, B.A. Matter, D.R. Powell, J. Am. Chem. Soc. 119 (1997) 11817.

[27] M.A. Bennett, H. Jin, A.C. Willis, J. Organomet. Chem. 451 (1993) 249.

[28] S.Y. Liou, M. Gozin, D. Milstein, J. Chem. Soc., Chem. Commun. (1995) 1965.

[29] G. Jia, H.M. Lee, I.D. Williams, J. Organomet. Chem. 534 (1997) 173.

[30] B.L. Shaw, J. Organomet. Chem. 200 (1980) 307.

[31] E. Farnetti, M. Graziani, in: A.F. Noels, M. Graziani, A.J. Hubert (Eds.), Metal Promoted Selectivity in Organic Synthesis, Kluwer Academic Publishers, Dordrecht, pp. 191–205.